Received: 12 February 2023 | Revised: 13 July 2023 | Accepted: 10 September 2023

DOI: 10.1002/ep.14293

ENVIRONMENTAL PROGRESS & SUSTAINABLE ENERGY

ORIGINAL RESEARCH

Sustainable Energy

Performance optimization of solar pump operating by PV module

Vineet Singh[1] | Vinod Singh Yadav[2] | Vaibhav Trivedi[1] | Manoj Kumar Singh[3]

[1]Department of Mechanical Engineering, School of Engineering & Technology, IFTM University, Moradabad, India

[2]Department of Mechanical Engineering, NIT, Srinagar, India

[3]Department of Mechanical Engineering, FET, MJP Rohilkhand University, Bareilly, India

Correspondence
Vineet Singh, Department of Mechanical Engineering, School of Engineering & Technology, IFTM University, Moradabad, Uttar Pradesh, India.
Email: vineetpsh@gmail.com

Funding information
Ministry of Education, India, Grant/Award Number: 1-5736521897; collaborative project scheme (CRS); NATIONAL PROJECT IMPLEMENTATION UNIT (NPIU)

Abstract

In this research article, the objective of the work is to maximize the performance of solar pump based on input variables. The solar panel and motor pump set are the important parts of solar pump. The overall performance of the solar pump has been depending on the performance of solar panels and motor pump set. The tilt angle, surface azimuth angle, module temperature and speed of motor are most important input parameters on which whole performance of solar pump depends. So, for fulling these objectives a 5 hp (horsepower) solar pump has been installed in FET MJP Rohilkhand University, Bareilly located at 28.36° N, 79.43° E. The experimental data of output parameters at the different settings of input parameters and data generated by model equations have been optimized by the Response Surface Methodology (RSM) tool of Design of Experiments (DOE). The optimum setting of input parameters are Tilt Angle (TA) (36.22°), Surface Azimuth Angle (SA) (−1.26°), Module Temperature (MT), and speed of the motor (2169.69 RPM). On the optimum setting of input parameters, the values of the response are maximum Solar Flux (SF) (762 W/m^2), maximum power output (3661.4578 W), minimum discharge (19.2681 m^3/h), head developed (55.17 m), maximum motor efficiency (90.7488%), maximum exergetic efficiency (15.3799%), minimum Levelized cost of electricity (LCOE) (0.0361 $/KWh), maximum panel efficiency (17.1774%) and maximum overall efficiency (15.0117%).

KEYWORDS
exergy, levelized cost of electricity, solar panel, solar power water pumping system, surface azimuth angle, tilt angle

1 | INTRODUCTION

A total of 58% of the Indian population depends on agriculture. Irrigation in agriculture depends on the fossil fuels energy supply.[1] Apart from this, agriculture continues to be a primary barrier to achieving total water, energy, and food security.[2] One of the most important factors in agriculture is water. During dry seasons, the most difficult aspect of irrigation is collecting the required amount of water. As a result, farmers mostly employ power-generated water pumps to irrigate crops.[3] The population of India uses an alternating current-driven

Abbreviation: Acronym, Description; ANOVA, Analysis of variance; DOE, Design of experiment; GA, Genetic algorithm.; HOMER, Hybrid optimization of multiple energy resource; hp, Horse power; LCOE, Levelized cost of energy; LPM, Liter per minute; MMRO, Manta-ray optimization; MPPT, Maximum power point tracking; MSE, Mean square error; MT, Module temperature; PMDC, Permanent magnet direct current; PV, Photovoltaic; PVWPS, Photovoltaic water pumping system; RCCD, Rotatable central composite design; RPM, Revolution per minute; RSM, Response surface methodology; SA, Surface azimuth angle; SF, Solar flux (W/m^2); SPWPS, Solar photovoltaic water pumping system; TA, Tilt angle.

TABLE 1 Optimization techniques/Methods used in solar photovoltaic pump.

S. NO.	Optimization techniques	Input variables	Output variables	Authors
1	RSM	Solar panel Tilt Angle (TA) and Surface Azimuth Angle (SA)	Solar flux, solar panel efficiency, overall efficiency, power output.	[32]
2	RSM	Module temperature, water inlet velocity, solar flux	Optimize the solar panel efficiency and exergy.	[33]
3	GA	Solar Flux, Speed of motor, and discharge of the pump	Maximize the power output and minimize the LCOE	[34]
4	GA	Solar panel tilt angle and the discharge	Maximize the annual profit	[35]
5	Maximum Power Point Tracker (MPPT) and DC to DC power converter. The MATLAB Simulink circuit is used for optimizing the system	Solar flux and PV module temperature.	Maximizing the power output, subsystem efficiency, and power output.	[36]
6	Swarm Optimization Technique	Tilt angle and the discharge of the pump	Minimize the Levelized Cost Of Electricity (LCOE)	[37]
7	GA	Solar Flux, wind velocity, and air temperature	Minimize the cost	[38]
8	GA and Particle Swarm Algorithms	The capacity of prime mover, number of prime movers, and the partial load	Minimum investment cost and the maximum efficiency of the system	[39]
9	HOMER software is used for determining the optimum tilt angle	Optimum tilt angle	Minimizing the total cost	[40]
10	HOMER	Optimum discharge and the speed of the pump	Load demand, available resources, and the cost of energy	[41]
11	Manta Ray (MMRO) optimization Technique	NA	Hybrid system (Diesel generator, pumped hydro and PV modules) cost has to be minimized.	[28]
12	Particle Swarm Optimization	PV capacity, Stored water capacity, and Battery storage capacity	Minimizing the total cost	[42]

motor to pump water from wells and rivers. The typical pumping system has the benefit of being simple to install, but it has several drawbacks, such as regular equipment maintenance, refueling, and a lack of diesel supply.[4] Furthermore, the usage of fossil fuels, such as diesel has a negative influence on the environment, notably the release of greenhouse gasses, such as carbon dioxide (CO_2) into the atmosphere.[5] To address these issues, researchers and scientists are attempting to develop an efficient solution based on renewable sustainable energy that is both environmentally benign and financially effective.[6]

The continual depletion of traditional energy sources, as well as its environmental consequences, has sparked interest in using RESs to power water pumping systems, such as solar-photovoltaic,[7] solar-thermal,[8] wind energy,[9] producer gas,[10] and biomass sources.[11] India is lie in the area of the world of rich solar energy sources. As a result, there is a significant opportunity to use solar energy in agriculture for pumping water. SPWPS is one such application that can help meet agricultural and drinking water demands in rural and distant places where grid energy is not easily accessible. SPWPS is environmentally friendly, needs no maintenance, and has no fuel costs.[12] The water flow rate is affected by solar flux and the size of the PV array. Furthermore, tanks can be utilized for water storage instead of batteries for power storage for cost savings.[13]

With increased awareness of the world's increasing energy dilemma, SPWPS has been a topic of study for research. Several studies have been conducted across the world to explore and assess the performance of SPWPS. In Algeria, SPWPS has enormous potential for drinking and agriculture purposes. Amina et al.[14] suggested a solo solar water pumping system concept. The effect of the optimum design of a PV water pumping system, as well as the influence of the metrological circumstances of Adrar, Algeria, on the system's performance, were investigated in this study. Mohanlal et al.[15] evaluated the performance of a stand-alone directly connected SPVWPS with PMDC, series, and shunt motors coupled with centrifugal and constant loads at various sun intensities and cell temperatures. They discovered that a PMDC motor combined with a centrifugal pump outperforms a DC series and shunt motor. When compared to DC shunt and series motors, PMDC works much of the day due to its higher starting torque, even at low solar intensities. Chauncey et al.[16,17] conducted a similar study and reported the development of SPWPSs in India. They proposed that SPWPSs are practical for a 500-person community. Allouhi et al.[18] investigated the ideal configuration of a PV water pumping system to meet the residential water demands of five independent Moroccan buildings. Based on real water use data, a thorough strategy for optimum PV system design was given. In addition, system operation and energy analysis were carried out following hourly meteorological conditions. They demonstrated that their methods were less expensive than traditional water pumping systems. Kerry A. Sado et al.[19] explore a DC SPWPS for

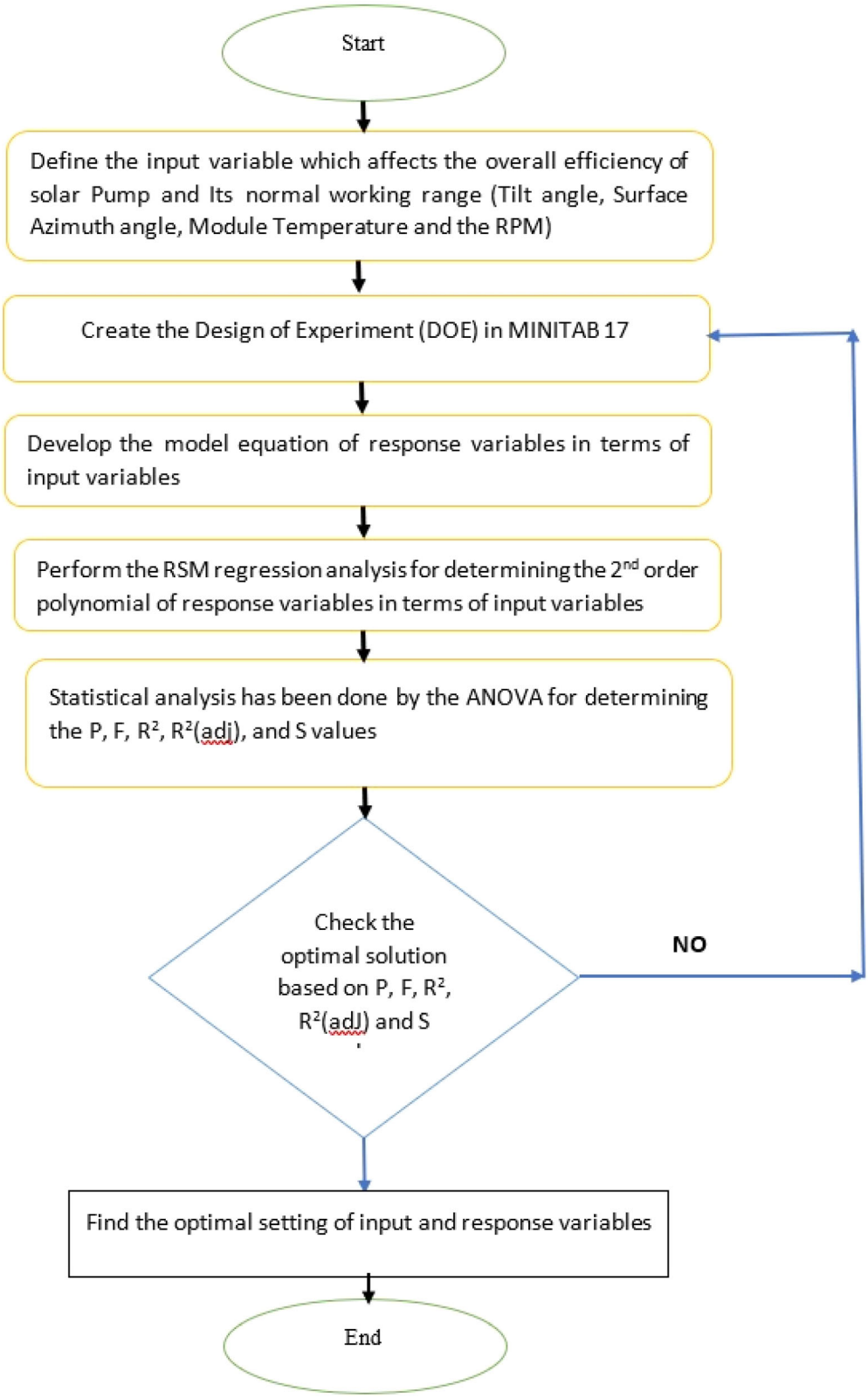

FIGURE 1 Flow chart of RSM.

Irrigation in Duhok City, taking into account the effect of optimal tilt angle, on power output, current, and water discharge. In a laboratory in Greece, Kaldellis et al.[20] investigated the efficacy of PV water pump systems and their capacity to move water for agriculture and drinking water supply, particularly in remote portions of the grid. Their empirical findings indicated that the PVWPS might be environmentally

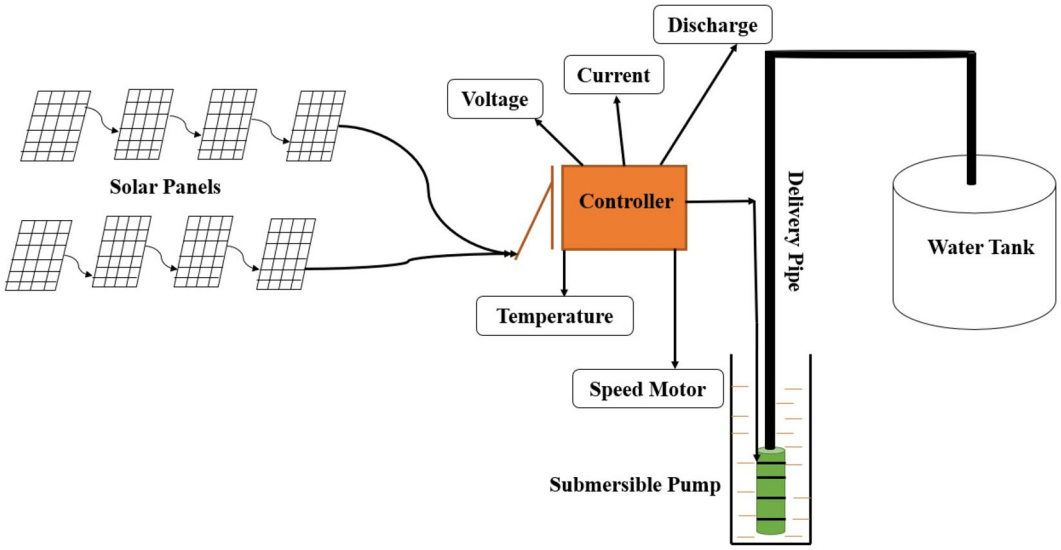

FIGURE 2 Schematic diagram of the solar pump with grid supply.

TABLE 2 Solar pump components and properties.

Number of solar panels	15
Solar panel power (kW)	5
Size of the pump (kW)	3.73 (AC submersible pump)
Tilt angle	28°N
Solar azimuth angle	0°

benign. Waddington et al.[21,22] investigated the relationship between flow rate and solar radiation using a low-head centrifugal pump. W.G. Le Roux[23] discovered that any fixed solar at the latitude of the place could capture the 98% insolation supplied by the Sun. This data is used for designing the solar pump.

Despite the benefits of photovoltaic energy, it has several disadvantages due to its intermittent nature. As a result, a precise PV power forecast is necessary. The photovoltaic energy is mostly determined by TA and SF.[24] As a result, it may be predicted using weather data estimates. The PV power is then calculated using a mathematical model of the panel.[25] The solar geometry, such as the solar declination angle, the hour angle, the tilt angle, the surface azimuthal angle, the location coordinate, the modular temperature, and the solar elevation, influences the physical models. The Sun releases 1.8×10^{11} MW of energy on the earth's surface which is quite large than the world energy demand.[26] The optimum size and solar panel arrangement very much affect the outlet discharge and power output of the solar pump. One study has been conducted to find out the optimum configuration of PV modules for the solar water pumping system. In this study, the five configurations (4S × 2P, 5S × 2P, 7S, 8S, and 3S × 2P) have been tested on the varying head of the solar pump. Finally, it was concluded that 5S × 2P gives the maximum discharge in winter and the 8S configuration gives the maximum discharge in the summer season (Sontake et al.[27]).

The solar panel temperature plays a very important role in the performance of the solar panel. The power output and efficiency of solar pumps have been reduced due to an increase in the temperature of solar panels. A Research has been conducted on a 2 hp solar pump experimentally for knowing the effect of water cooling on the top, bottom, and sides of the solar panel. The system has been analyzed and debated to know the effect of water cooling on discharge, panel efficiency, and system efficiency. The findings of the system show that top and bottom cooling with jute considerably improves the performance parameters of the SPWPS.[28]

The long-term performance of the solar pump has been determined by a simple algorithm.[29–31] In which a non-linear correlation has been developed between discharge and solar flux. Finally, the output results of the discharge at different values of solar flux have been experimentally validated with 5% accuracy.

The solar photovoltaic pumping system mainly consists of three parts one is the PV module 2nd is the impedance matching (Boost converter + MPPT) and 3rd have the motor pumping system.[36] Most of the time previous research focuses on improving the performance of solar photovoltaic pumps by enhancing the efficiency of PV modules, changing the electric circuit, and changing different types of pumps. The study also focused on the performance optimization of solar pumps based on the tilt angle. Table 1 shows the methods used for optimization with the input variables but very less study focuses on the optimization by Response Surface Methodology (RSM) with the four most important input variables. As per my knowledge, this is considered to be a big research gap and novelty of this work.

The overall efficiency of the solar photovoltaic pumping system is the multiplication of the efficiency of the solar panel and the efficiency of the motor pump system. So, for improving the overall performance of the solar pumping system solar panel and submersible pumps must give the maximum performance. The solar panel efficiency is maximum when it works at an optimum tilt angle, surface azimuth angle, and optimum temperature of the panel. The motor pump system efficiency depends on the speed of the pump and it is

FIGURE 3 Schematic diagram of the solar photovoltaic pumping system.

FIGURE 4 Motor pump setup installed below the roof of the university.

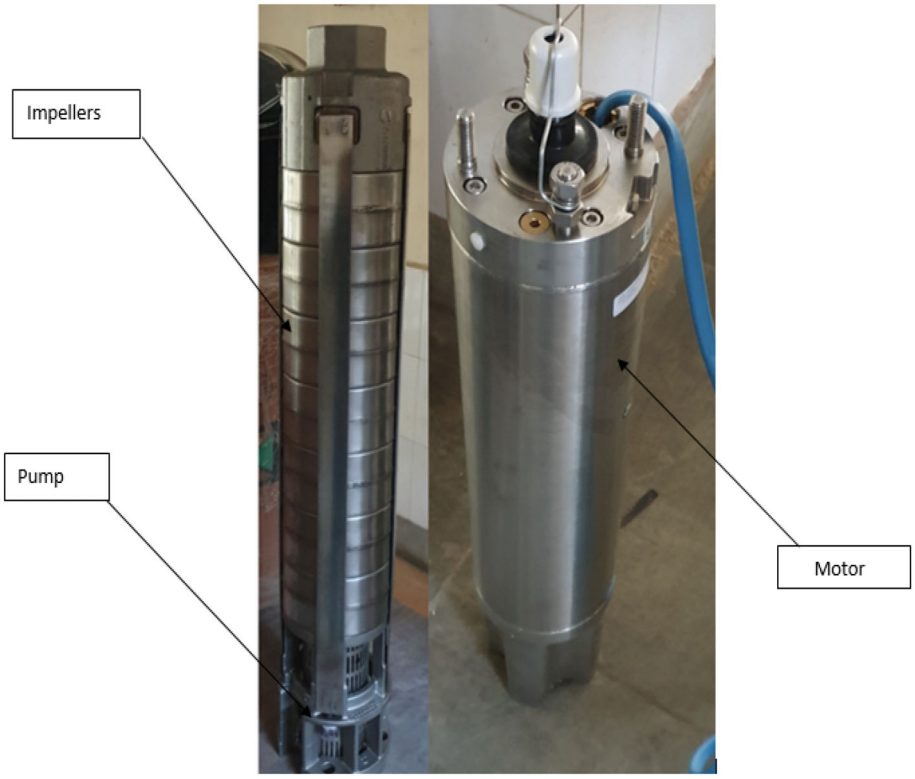

maximum at some optimum range of the speed of the motor. So, in this study, the four input variables (TA, SA, MT, and speed of the motor) have to be determined at maximum efficiency, exergy, and minimum LCOE.

To the best of the author's knowledge, no research has focused on developing a regression model to forecast the influence of solar physical geometry, such as tilt angle (TA), the surface azimuthal angle (SA), modular temperature (MT), rpm of the motor on solar power water pump systems (SPWPS) using RSM. The uniqueness and authenticity of this study are that it is the first to create a polynomial model to anticipate SPWPS productive outputs. The primary goal of this research is to give a complete assessment of SPWPS operation and performance from technical, economic, and environmental perspectives. The purpose of this work is to investigate the effects of four input factors that have the greatest influence on SPWPS output, in the range of namely tilt angle (4 to 62°), the surface azimuthal angle (−10 to 10°), modular temperature (20 to 60°C), rpm of motor (1600 to 2400 rpm). The output responses for this study are solar flux, power output, discharge (m^3/h), head required, motor efficiency (%), exergy, Levelized cost of energy (LCOE), panel efficiency (%), and

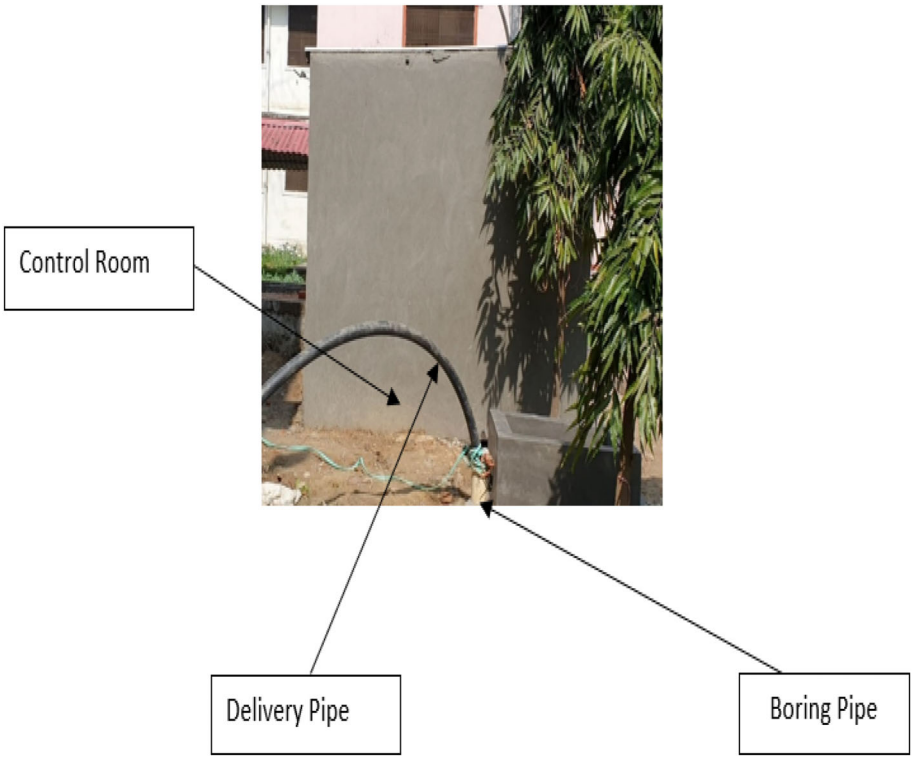

FIGURE 5 Control room installed below the roof of the university.

TABLE 3 Range of selected input variables.

Input parameters	Coded levels				
	−2	−1	0	1	2
Tilt angle (degree)	4	16	28	40	62
Surface azimuth angle (degree)	−10	−5	0	5	10
Module temperature (°C)	20	30	40	50	60
RPM	1600	1800	2000	2200	2400

overall efficiency (%). The following are the steps used for the optimization of SPWPS by RSM presented in Figure 1.

2 | SOLAR POWER WATER PUMP SYSTEM

2.1 | Working principle of SPWPS and experimental setup

Figure 2 represents the full schematic diagram of the SPWPS project located at 28.36°N and 79.43° E, at FET, MJP Rohilkhand University, and Bareilly. For increasing the revenue of farmers, the solar pump project is used for supplying the water of 0.25 ha farm for irrigation, and the remaining time supplying the power to the grid. The 5 hp pump has to be selected for irrigation of a 0.25 ha farm size, the 3 days' time will be spent for one-time irrigation in a month and the remaining time of the month solar panels will be used for supplying the electricity to the grid. The total time of growing to maturity of the wheat is 120 days of which every month one-time water is required for irrigation. In a year pump remain busy for 36 days for supplying the water and the remaining 329 days will supply the electricity to the grid. The list of components used for the experimental setup is given in Table 2.

The experimental test rig is shown in Figure 2 and its main components are shown in Figures 3 and 4. A total of 15 modules have been used in the system and all modules are connected in series. The specification of the PV module is given in Ref.32. The PV modules generate the DC power which is further converted into AC power by the solar pump controller, the specification of the controller is given in Ref.32. The solar pump has a display system that shows the reading of all the components. It shows the temperature of the module, atmosphere temperature, output current, voltage, speed of the motor pump, and discharge of the pump. The controller has been mounted on the structure of the solar panel for minimizing the DC-to-DC loss. The controller supplied the AC power to the motor pump set. The brushless AC motor operates at 380 V, 9 A, and 2860 RPM and requires 5 hp power. A multi-stage submersible pump is used with the combination of the motor pump, which develops the pumping capacity of 200 LPM at a pumping head of 50 m. The specifications of the solar pump controller

TABLE 4 Actual values of independent variables along with their responses.

S.N.	TA	SA	MT	RPM	Solar Flux (W/m^2)	P_O (W)	Q (m^3/h)	H_R (m)	η_m (%)	Φ (%)	LCOE ($/kWh)	η_P (%)	η_O (%)
1	40	5	50	2200	781	3307	17	51	94	14	0.038512	14.52	14
2	28	0	40	2000	708	3198	17	50	77	15	0.04866159	15.49	12
3	28	0	40	2000	711	3211	17	50	77	15	0.04865135	15.49	12
4	28	0	60	2000	715	2850	15	47	77	13	0.039318	13.68	11
5	40	−5	50	1800	687	2933	15	48	62	14	0.03967	14.65	9
6	16	−5	50	1800	855	3650	19	55	62	14	0.037647	14.65	9
7	40	5	50	1800	775	3315	17	51	62	14	0.038584	14.68	9
8	16	−5	30	2200	849	4044	21	59	93	15	0.037715	16.34	15
9	16	−5	50	1800	851	3641	19	55	62	14	0.037692	14.68	9
10	28	0	40	1600	703	3175	17	50	49	15	0.039468	15.49	8
11	28	0	40	2000	709	3202	17	50	77	15	0.039393	15.49	12
12	28	0	20	2000	706	3563	19	54	77	16	0.03943	17.31	13
13	16	5	30	2200	857	4113	22	60	93	16	0.037624	16.46	15
14	28	0	40	2000	710	3207	17	50	77	15	0.04855132	15.49	12
15	28	0	40	1600	712	3216	17	50	49	15	0.039355	15.49	8
16	40	5	30	1800	785	3753	20	56	62	16	0.038464	16.40	10
17	16	5	50	2200	852	3607	19	54	93	14	0.037681	14.52	14
18	4	0	40	2000	778	3514	18	53	77	15	0.038548	15.49	12
19	16	5	50	1800	848	3553	19	54	62	14	0.037727	14.37	9
20	28	−10	40	2000	782	3532	19	54	77	15	0.0384	15.49	12
21	28	10	40	2000	853	3853	20	57	77	15	0.037669	15.49	12
22	16	−5	50	2200	850	3614	19	54	93	14	0.037704	14.58	14
23	28	0	40	2000	707	3193	17	50	77	15	0.04864132	15.49	12
24	28	0	40	2000	709	3202	17	50	77	15	0.04865133	15.49	12
25	40	−5	30	2200	689	3270	17	51	94	15	0.039645	16.28	15
26	40	5	30	2200	772	3664	19	55	93	15	0.03862	16.28	15
27	40	−5	50	2200	693	2934	15	48	94	14	0.039594	14.52	14
28	16	5	30	1800	854	4083	21	60	62	16	0.037658	16.40	10
29	28	0	40	2000	703	3175	17	50	77	15	0.04866132	15.49	12
30	40	−5	30	1800	691	3304	17	51	62	16	0.039619	16.40	10
31	62	5	50	2200	594	2515	13	44	94	14	0.040887	14.52	14

and the specifications of instruments used in experimentation are given in Ref.32 Figure 5 represents the solar pump delivery pipe and control room on the ground below the roof of the university.

3 | RESPONSE SURFACE METHODOLOGY APPROACH

Response surface methodology is an optimization tool used in the design of experiments (briefly explained by the flow chart in Figure 1). The goal is to maximize the output responses that are impacted by the number of input variables. Many academics have utilized response surface methods to optimize process parameters and have created a regression equation to predict the response.[43] By taking the input parameters into account, a second-order polynomial regression equation, as indicated in Equation (1), is utilized to predict the response.[44]

$$Y = \beta_\circ + \sum_{i=1}^{k} \beta_i x_i + \sum_{i=1}^{k} \beta_{ii} x_i^2 + \sum_{j \geq 1}^{k} \beta_{ij} x_i x_j + \varepsilon \quad (1)$$

where Y is the response, $\beta_\circ$ is the average of the replies, and β_i, β_{ii}, and β_{ij} are the response coefficients The second, third, and fourth terms, respectively, reflect linear, higher-order, and interaction effects and ε is the error or noise in the system.

The analysis of variance (ANOVA) approach is one of RSM's useful characteristics for developing an appropriate model between the response and independent variables. For proper 2nd order polynomial response modeling, the RCCD (Rotatable Central Composite Design) approach is

TABLE 5 *P*-value and *F* value for checking the effectiveness of the regression analysis on SF and power.

		SF (solar flux)				Power			
Sources	**DF**	**Adj. SS**	**Adj. MS**	***F*-value**	***P*-value**	**Adj. SS**	**Adj. MS**	***F*-value**	***P*-value**
Model	14	133,656	9546.9	7.14	0.000	3,584,518	256,037	9.59	0.000
Linear	4	4575	1143.7	0.86	0.511	82,139	20,535	0.77	0.561
TA	1	847	847.2	0.63	0.438	17,435	17,435	0.65	0.431
SA	1	740	740.4	0.55	0.468	15,935	15,935	0.60	0.451
MT	1	127	126.9	0.09	0.762	516	516	0.02	0.891
RPM	1	2350	2350.1	1.76	0.203	39,869	39,869	1.49	0.239
Square	4	36,637	9159.3	6.85	0.002	735,848	183,962	6.89	0.002
TA*TA	1	36	36.0	0.03	0.872	521	521	0.02	0.891
SA*SA	1	33,894	33893.6	25.36	0.000	687,145	687,145	25.73	0.000
MT*MT	1	1961	1960.6	1.47	0.243	37,581	37,581	1.41	0.253
RPM*RPM	1	3958	3957.7	2.96	0.105	72,086	72,086	2.70	0.120
2-way Interaction	6	8643	1440.6	1.08	0.416	187,500	31,250	1.17	0.370
TA*SA	1	3272	3271.9	2.45	0.137	73,325	73,325	2.75	0.117
TA*MT	1	1915	1914.6	1.43	0.249	12,516	12,516	0.47	0.503
TA*RPM	1	1021	1021.4	0.76	0.395	32,623	32,623	1.22	0.285
SA*MT	1	1474	1474.0	1.10	0.309	51,326	51,326	1.92	0.185
SA*RPM	1	411	410.6	0.31	0.587	5938	5938	0.22	0.644
MT*RPM	1	802	802.3	0.60	0.450	16,825	16,825	0.63	0.439
Error	16	21,388	1336.8	–	–	427,309	26,707	–	–
Lack of Fit	8	21,299	2662.3	238.36	0.000	425,592	53,199	247.95	0.000
Pure Error	8	89	11.2	–	–	1716	215	–	–
Total	30	15,504	–	–	–	4,011,826	–	–	–

typically utilized. For 2nd order response modeling, the responses specify the best approximation within the stated range of all input variables. The required number of these experiments at different four input settings with five levels is given in Table 3. As a result, the system modeling must affect a reliable forecast for the output response at sites of interest, β_i, and RCCD recognizes this. A conventional RCCD module is utilized in this experiment, with the system having four input variables.[35]

3.1 | Application of RSM

The influence of four elements on the efficiency of SPWPS is investigated in this research, in order of importance: TA, the SA, MT, speed of the motor (rpm) on SPWPS. It is decided to use the RCCD model with the face as the focal point. The following correlation is used to determine the number of points or runs.[45]

$$n = 2^p + 2p + c \quad (2)$$

where n is the total set of data points, p is designated as several input variables, and c denotes the number of replications at the axial points. The total 31 data sets at four input variables are given in Table 3. Therefore, total experiment observations were 31 according to Equation (2) as shown in Table 4. In Table 4 values of responses like solar flux, power output, discharge, head, motor efficiency, exergy efficiency, LCOE, panel efficiency and overall efficiency have in represented for all 31 data sets. Based on these 31 data sets ANOVA form the 2nd degree polynomial regression equation of responses in terms of four input variables. Equations 4 to 11 represents the regression equation of responses in terms of input variables.

3.2 | Analysis of variance

An analysis of variance (ANOVA) is used to determine the suitability of the formulated polynomial model (Tables 5–9). The Tables 5–9 represents the Degree of Freedom (DF), adjusted Sum of Squares (adj. SS), adjusted Mean Sum of Squares (adj. MS), *F* and *P* values for all response variables like solar flux, power output, discharge, motor efficiency, solar panel efficiency, exergy and LCOE. Degree of Freedom represents the frequency of input variables in second order response model regression equations. These parameters have been calculated for all terms represented in the second order model equations of the response variables due to that in each table values are changes as per the dependency of the response variables on the input variables. The *F*-value is a test

TABLE 6 *P*-value and *F* value for checking the effectiveness of the regression analysis on discharge and head.

		Discharge				Head			
Sources	**DF**	**Adj. SS**	**Adj. MS**	***F*-value**	***P*-value**	**Adj. SS**	**Adj. MS**	***F*-value**	***P*-value**
Model	14	104.456	7.4612	12.26	0.000	376.748	26.9106	9.04	0.000
Linear	4	2.287	0.5717	0.94	0.466	8.089	2.0223	0.68	0.616
TA	1	0.708	0.7080	1.16	0.297	0.198	0.1976	0.07	0.800
SA	1	0.291	0.2913	0.48	0.499	2.889	2.8893	0.97	0.339
MT	1	0.010	0.0098	0.02	0.901	0.211	0.2114	0.07	0.793
RPM	1	1.025	1.0252	1.68	0.213	4.287	4.2874	1.44	0.248
Square	4	18.523	4.6307	7.61	0.001	90.164	22.5409	7.57	0.001
TA*TA	1	0.334	0.3342	0.55	0.469	0.004	0.0044	0.00	0.970
SA*SA	1	17.229	17.2290	28.31	0.000	83.984	83.9841	28.21	0.000
MT*MT	1	0.781	0.7812	1.28	0.274	6.919	6.9195	2.32	0.147
RPM*RPM	1	1.832	1.8322	3.01	0.102	7.553	7.5532	2.54	0.131
2-way Interaction	6	5.687	0.9478	1.56	0.223	19.356	3.2261	1.08	0.413
TA*SA	1	2.661	2.6613	4.37	0.053	5.265	5.2653	1.77	0.202
TA*MT	1	0.489	0.4886	0.80	0.384	0.240	0.2400	0.08	0.780
TA*RPM	1	0.839	0.8392	1.38	0.257	1.617	1.6174	0.54	0.472
SA*MT	1	1.205	1.2053	1.98	0.178	9.130	9.1299	3.07	0.099
SA*RPM	1	0.115	0.1146	0.19	0.670	0.790	0.7904	0.27	0.613
MT*RPM	1	0.382	0.3825	0.63	0.440	2.507	2.5069	0.84	0.372
Error	16	9.737	0.6086	*	*	47.639	2.9775	*	*
Lack of Fit	8	9.737	1.2172	*	*	47.639	5.9549	*	*
Pure Error	8	0.000	0.0000	*	*	0.000	0.0000	*	*
Total	30	114.194		*	*	424.387	*	*	*

statistic that is used to see if the model is missing words that contain the experiment's components. The lack-of-fit test includes these words as well if blocks are removed from the model in a stepwise manner. Minitab calculates the *p*-value using the *F*-value, which you use to decide if the test is statistically significant. A big enough *F*-value denotes statistical significance.[46]

If the *p*-value is less than or equal to the significance threshold, the model is said to explain response variation. The calculated *P* values for all models is very near to 0.00 shows the null hypothesis is neglected since the values of *p* is less than 0.05. We cannot infer that the model explains variance in the response if the *p*-value is larger than the significance level.[44,47]

The standard deviation of the distance between the data values and the fitted values is denoted by the letter S as shown in Table 10. S is the response's unit of measurement. The percentage of variance in the response described by the model is known as R^2. It is computed as 1 min the ratio of the error sum of squares to the overall sum of squares (which is the variance that is not explained by the model) (which is the total variation in the model). The proportion of variance in the response described by the model, adjusted for the number of predictors in the model versus the number of observations, is known as adjusted R^2. The adjusted R^2 is computed as 1 min the mean square error (MSE) to the mean square total ratio (total MS). The addition of constants in the regression model always increases the values of the R^2 but the adj. R^2 value not always increases since it depends on the number of degrees of freedom. The formula for calculating predicted R^2 is the same as methodically deleting each observation from the data set, evaluating the regression equation, and measuring how well the model predicts the deleted observation. The predicted R^2 value might be anything between 0% and 100 and it is calculated for the new data sets of the input variables in some other ranges.

3.3 | Optimization plot

The combined desirability (D) forecasts how a set of overall objectives will be optimized by the input elements. Combined desirability varies from 0 to 1 for optimization research, with a greater value always favoring better optimization. The combined desirability (Figure 4) was found to be 0.7560 in this study. This study demonstrates that RSM models may be used to determine the optimal system operating variables that result in the best pump performance and efficiency metrics. As a result, while assigning optimization parameters during numerical optimization, the criteria for solar flux, power output, discharge (m^3/s), motor efficiency (%), exergy efficiency, solar panel efficiency,

TABLE 7 *P*-value and *F* value for checking the effectiveness of the regression analysis on motor efficiency and exergy.

		η (Motor)				Exergy			
Sources	**DF**	**Adj. SS**	**Adj. MS**	***F*-value**	***P*-value**	**Adj. SS**	**Adj. MS**	***F*-value**	***P*-value**
Model	14	5778.11	412.722	11006.11	0.000	17.0393	1.21709	51.24	0.000
Linear	4	0.63	0.157	4.17	0.017	0.4512	0.11280	4.75	0.010
TA	1	0.59	0.590	15.73	0.001	0.0079	0.00786	0.33	0.573
SA	1	0.01	0.005	0.15	0.707	0.0021	0.00211	0.09	0.769
MT	1	0.04	0.044	1.18	0.294	0.3011	0.30114	12.68	0.003
RPM	1	0.05	0.055	1.46	0.245	0.0409	0.04088	1.72	0.208
Square	4	13.78	3.444	91.84	0.000	0.5259	0.13148	5.54	0.005
TA*TA	1	0.03	0.034	0.90	0.356	0.0099	0.00991	0.42	0.527
SA*SA	1	0.02	0.016	0.42	0.524	0.0009	0.00085	0.04	0.852
MT*MT	1	0.02	0.016	0.42	0.524	0.3896	0.38958	16.40	0.001
RPM*RPM	1	13.48	13.478	359.42	0.000	0.1446	0.14461	6.09	0.025
2-way Interaction	6	0.87	0.146	3.89	0.014	0.8421	0.14034	5.91	0.002
TA*SA	1	0.05	0.053	1.41	0.252	0.0561	0.05610	2.36	0.144
TA*MT	1	0.06	0.065	1.73	0.207	0.0609	0.06085	2.56	0.129
TA*RPM	1	0.62	0.622	16.60	0.001	0.0561	0.05610	2.36	0.144
SA*MT	1	0.08	0.082	2.19	0.158	0.0723	0.07231	3.04	0.100
SA*RPM	1	0.03	0.031	0.83	0.376	0.0554	0.05535	2.33	0.146
MT*RPM	1	0.08	0.082	2.19	0.158	0.4760	0.47598	20.04	0.000
Error	16	0.60	0.037			0.3800	0.02375		
Lack of Fit	8	0.60	0.075	*	*	0.3800	0.04750	*	*
Pure Error	8	0.00	0.000			0.0000	0.00000		
Total	30	5778.71				17.4194			

and overall efficiency to be maximized and the LCOE, head require set to be minimum.

Figure 6 displays RSM optimizer results. The optimum solar flux, power output, discharge (m^3/s), head required, motor efficiency (%), exergy, LCOE, panel efficiency (%), and overall efficiency (%) values are 90.74%, 15.37 kJ/K, 0.0361, 17.1774%, and 15.01% respectively, with the corresponding optimum operational factors of TA (36.22°), SA (−1.260°), MT (21.10°C), and rpm (2169).

4 | RESULTS AND DISCUSSIONS

In the current investigation, the impacts of input factors, such as TA, the SA, MT, and rpm of the motor on SPWPS were investigated. Table 7 displays the experimental responses of 31 runs in the design matrix, as well as the points on RSM-fitted models that correspond to them. 3-D surface view plots and accompanying contour plots were created using the four independent components. Two items were considered at a time in these plots, with the other two factors staying in the middle level and serving as hold parameters.

4.1 | Interactive effect of various input factors on SF

$$I_t = 1614 + 6.11\alpha + 16.4\lambda + 3.6\,T_m - 0.0072\,\alpha^2 + 1.409\,\lambda^2 + 0.0847\,T_m^2 + 0.234\,\alpha\lambda - 0.0909\,\alpha T_m - 0.200\,\lambda T_m \quad (3)$$

Figure 7 shows that the solar flux is enhanced by increasing the surface azimuth angle from 0 to 10° and reduced by increasing the value of tilt angle since higher values of TA increase the incidence angle perpendicular to the plane of the solar panel, which reduces the normal component of radiation.[48] So lower tilt angle between 20 and 40° gives the maximum solar flux by holding the value of module temperature 21.1°C and speed of the motor 2169 rpm.

4.2 | Interactive effect of various input factors on power output

$$P_O = 7768 + 27.7\,\alpha + 76.1\,\lambda - 7.3\,T_m - 0.027\alpha^2 + 6.34\,\lambda^2 + 0.371T_m^2 + 1.107\,\alpha\lambda - 0.233\alpha T_m - 1.181\,\lambda\,T_m - 0.0197\,\lambda \quad (4)$$

TABLE 8 *P*-value and *F* value for checking the effectiveness of the regression analysis on LCOE and panel efficiency.

		LCOE				η_P			
Sources	**DF**	**Adj. SS**	**Adj. MS**	***F*-value**	***P*-value**	**Adj. SS**	**Adj. MS**	***F*-value**	***P*-value**
Model	14	0.000394	0.000028	4.20	0.004	20.2188	1.44420	742.57	0.000
Linear	4	0.000099	0.000025	3.68	0.026	0.1409	0.03521	18.11	0.000
TA	1	0.000000	0.000000	0.05	0.828	0.0076	0.00757	3.89	0.066
SA	1	0.000003	0.000003	0.46	0.508	0.0047	0.00466	2.40	0.141
MT	1	0.000013	0.000013	1.97	0.179	0.0962	0.09620	49.46	0.000
RPM	1	0.000087	0.000087	12.93	0.002	0.0073	0.00732	3.76	0.070
Square	4	0.000376	0.000094	14.05	0.000	0.0074	0.00185	0.95	0.461
TA*TA	1	0.000039	0.000039	5.77	0.029	0.0006	0.00060	0.31	0.585
SA*SA	1	0.000158	0.000158	23.58	0.000	0.0000	0.00000	0.00	0.991
MT*MT	1	0.000117	0.000117	17.47	0.001	0.0000	0.00005	0.03	0.875
RPM*RPM	1	0.000102	0.000102	15.20	0.001	0.0061	0.00615	3.16	0.094
2-way interaction	6	0.000012	0.000002	0.31	0.923	0.0608	0.01013	5.21	0.004
TA*SA	1	0.000001	0.000001	0.16	0.697	0.0075	0.00749	3.85	0.067
TA*MT	1	0.000005	0.000005	0.81	0.382	0.0143	0.01428	7.34	0.015
TA*RPM	1	0.000005	0.000005	0.67	0.424	0.0176	0.01757	9.03	0.008
SA*MT	1	0.000002	0.000002	0.30	0.589	0.0110	0.01099	5.65	0.030
SA*RPM	1	0.000001	0.000001	0.20	0.665	0.0098	0.00979	5.03	0.039
MT*RPM	1	0.000002	0.000002	0.25	0.621	0.0000	0.00003	0.02	0.904
Error	16	0.000107	0.000007			0.0311	0.00194		
Lack of fit	8	0.000034	0.000004	0.46	0.852	0.0307	0.00383	68.15	0.000
Pure error	8	0.000073	0.000009			0.0004	0.00006		
Total	30	0.000501				20.2499			

Figure 8 shows that the output power of the solar panel is decreasing when the tilt angle increases and is enhanced by increasing the SA at the fixed MT 21.1°C and the speed of the motor at 2169 rpm because increasing the tilt angle increases the module temperature of the solar panel which reduces the power output of the solar panel same verified by.[49]

4.3 | Interactive effect of various input factors on discharge

$$Q = 39.7 + 0.177\,\alpha + 0.325\,\lambda - 0.032\,T_m - 0.0233\,N - 0.00069\,\alpha^2 + 0.03176\,\lambda^2 + 0.00169\,T_m^2 + 0.000007\,N^2 + 0.00667\,\alpha\lambda - 0.00145\,\alpha T_m - 0.000094\,\alpha N - 0.00572\,\lambda T_m - 0.000087\,\lambda N - 0.000081\,T_m N \quad (5)$$

Figure 9 shows the surface plot of pump discharge versus the SA, TA, MT, and RPM of the system. Figure 9a represents the discharge variation with MT and speed of the motor by holding the value of TA 36.22° and SA −1.26°. Figure 8a shows that discharge is reduced when the MT value increases from 20 to 60°C since higher values of MT reduced the power developed by solar panels.[35] In Figure 9a if the RPM of the pump increases then the discharge increases due to the increased speed of the pump creating a higher suction pressure at the eye of the impeller.[50] Figure 9b shows that increasing the value of TA reduces the discharge due to the reduction of power developed and higher values of SA increase the discharge of the pump since power production increases by holding the value of MT 21.1°C and the speed of motor 2169 RPM.

4.4 | Interactive effect of various input factors on head

$$H_R = 101.8 + 0.093\,\alpha + 1.02\,\lambda - 0.148\,T_m - 0.0455\,N + 0.00008\,\alpha^2 + 0.0701\,\lambda^2 + 0.00503\,T_m + 0.000015\,N^2 + 0.00938\,\alpha\lambda - 0.00102\,\alpha T_m - 0.000130\,\alpha N - 0.01576\,\lambda T_m - 0.000228\,\lambda N - 0.000206\,T_m N \quad (6)$$

Figure 10a shows the variation of the developed head with the MT and speed of the motor by holding the values of TA 36.22° and SA −1.25°. The higher module temperature reduced the developed head by the pump at a constant value of TA 36.22° and SA −1.25° since the power developed by the solar panel was reduced. Figure 10a shows that if RPM increases then the head developed by the pump increases due to the increased speed of the pump.[27] Figure 10b shows the effect of variation of TA and SA on pump developed head by holding the values of MT 21.1°C and speed of motor

TABLE 9 *P*-value and *F* value for checking the effectiveness of the regression analysis on overall efficiency.

	η (Overall)				
Sources	**DF**	**Adj. SS**	**Adj. MS**	***F*-value**	***P*-value**
Model	14	145.164	10.3689	650.68	0.000
Linear	4	0.177	0.0443	2.78	0.063
TA	1	0.006	0.0065	0.41	0.533
SA	1	0.015	0.0154	0.96	0.341
MT	1	0.046	0.0464	2.91	0.107
RPM	1	0.155	0.1550	9.73	0.007
Square	4	0.967	0.2418	15.17	0.000
TA*TA	1	0.076	0.0758	4.75	0.045
SA*SA	1	0.022	0.0219	1.37	0.258
MT*MT	1	0.022	0.0219	1.37	0.258
RPM*RPM	1	0.853	0.8526	53.50	0.000
2-way Interaction	6	0.058	0.0097	0.61	0.718
TA*SA	1	0.010	0.0101	0.64	0.437
TA*MT	1	0.023	0.0233	1.46	0.244
TA*RPM	1	0.010	0.0101	0.64	0.437
SA*MT	1	0.015	0.0147	0.92	0.352
SA*RPM	1	0.005	0.0051	0.32	0.581
MT*RPM	1	0.015	0.0147	0.92	0.352
Error	16	0.255	0.0159		
Lack of fit	8	0.255	0.0319	*	*
Pure error	8	0.000	0.0000		
Total	30	145.419			

2169 rpm. The increasing magnitude of TA reduced the developed head since power developed by solar panels decreases and a reduction in values of SA enhances the head developed due to an increment in power output of the solar panel.

4.5 | Interactive effect of various input factors on η (Motor)

$$\eta_m = 7.40 - 0.1612\,\alpha + 0.045\,\lambda - 0.0677\,T_m - 0.00514\,N - 0.000220\,\alpha^2 + 0.00096\,\lambda^2 + 0.000241\,T_m^2 + 0.000020\,N^2 + 0.000941\,\alpha\lambda - 0.000529\,\alpha T_m - 0.000081\,\alpha N - 0.00149\,\lambda T_m - 0.000045\,\lambda N + 0.000037\,T_m N \quad (7)$$

Figure 11 represents the variation of motor efficiency with the MT, RPM, TA, and SA. Figure 11a shows that if the RPM of the motor increases, then the motor efficiency increases since at higher RPM head developed by the pump enhanced but the effect of module temperature is not significantly affecting the motor pump efficiency at constant values of TA 36.22° and SA −1.25°. Figure 11b shows that the efficiency of the solar pump will high in the region of higher values of TA and negative values of SA since power developed by the pump is enhanced.

4.6 | Interactive effect of various input factors on exergy

$$\phi = 16.30 + 0.0186\,\alpha - 0.0277\,\lambda - 0.1769 T_m + 0.00444\,N - 0.000119\,\alpha^2 + 0.00022\,\lambda^2 - 0.001194\,T_m^2 - 0.000002\,N^2 - 0.000969\,\alpha\lambda + 0.000513\,\alpha T_m - 0.000024\,\alpha N - 0.001402\,\lambda T_m + 0.000060\,\lambda N + 0.000090\,T_m N \quad (8)$$

The overall exergetic efficiency is the multiplication of the exergetic efficiency of the solar panel and the exergetic efficiency of the submersible pump. Figure 12a shows that if the magnitude of MT increases the exergetic efficiency is decreased since the increase in values of MT enhances the loss of heat in the atmosphere[49] and when RPM increased the exergetic efficiency is enhanced because the head developed by the pump increased. The low value of MT and high RPM give the maximum exergetic efficiency by holding the value of TA 36.22° and SA −1.25°. Figure 12b represents the variation of overall exergetic efficiency variation with SA and TA by holding the values of MT 21.1°C and RPM 2169. Figure 12b shows that increasing the value of TA reduced the overall exergetic efficiency due to a reduction in power output with increasing values of TA. In Figure 12b the overall efficiency is enhanced by increasing the values of SA due to an increase in power output. At low-value TA and high-value of SA, the overall exergetic efficiency is maximum.

TABLE 10 Assessment of model.

Model	SD (Standard deviation)	R^2	Adjusted R^2	Predicted R^2
SF	36.5617	86.21%	74.13%	10.78%
Power O/P	163.422	89.35%	80.03%	30.64%
Discharge	0.780116	91.47%	84.01%	51.64%
Head	1.72553	88.77%	78.95%	29.09%
η (Motor)	0.193648	99.99%	99.98%	99.92%
Exergy	0.154117	97.82%	95.91%	83.74%
LCOE	0.0025880	78.63%	59.92%	1.78%
η (Panal)	0.0441007	99.85%	99.71%	99.02%
η (Overall)	0.126236	99.82%	99.67%	98.91%

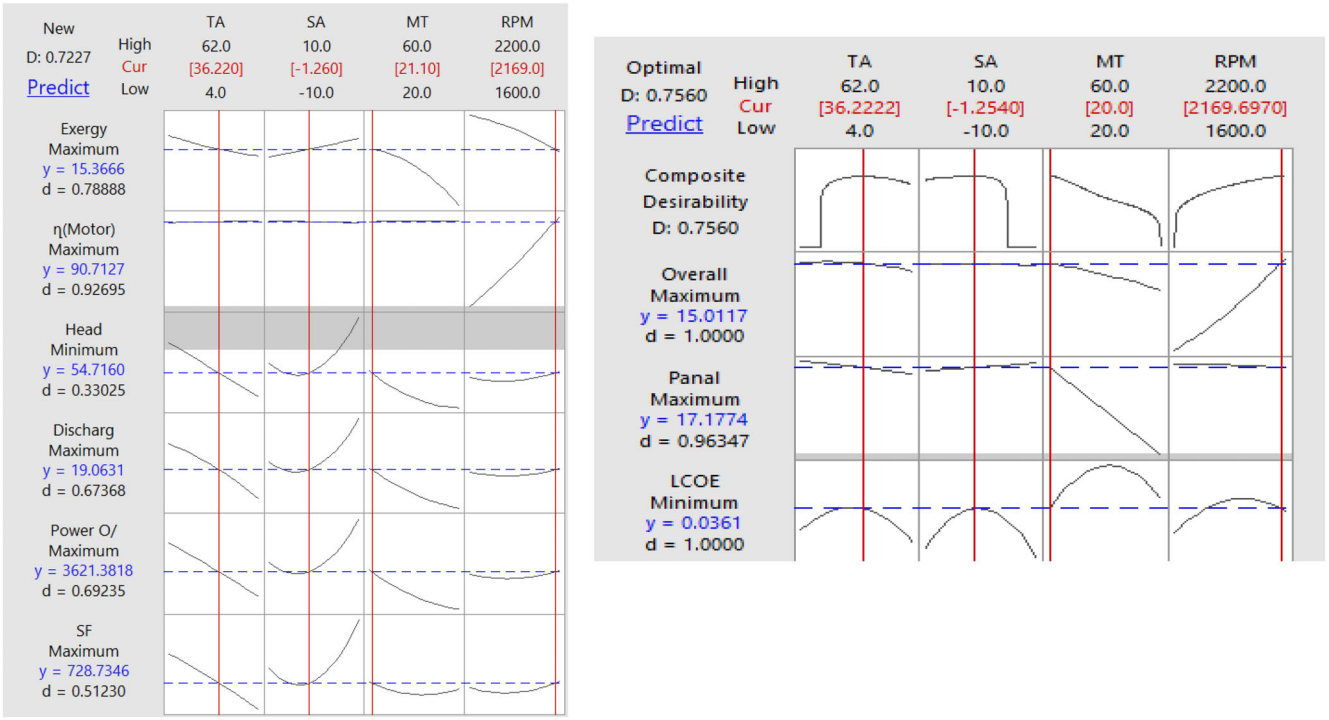

FIGURE 6 Optimization results plot.

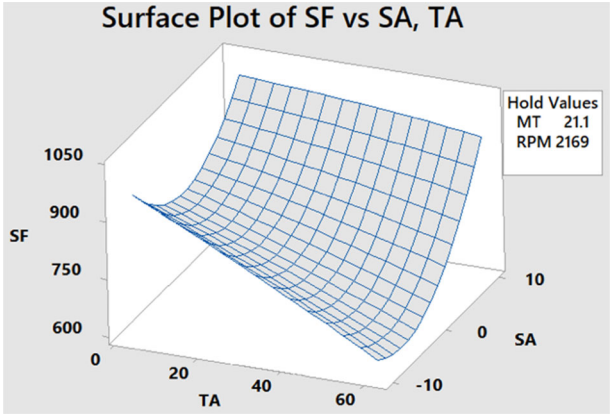

FIGURE 7 Variation of solar flux with the SA and TA.

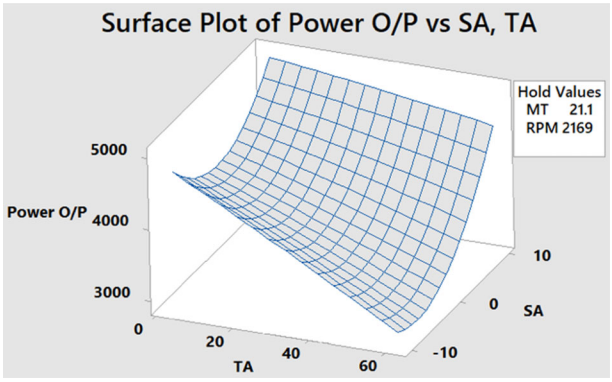

FIGURE 8 Variation of solar panel power output with the SA and TA.

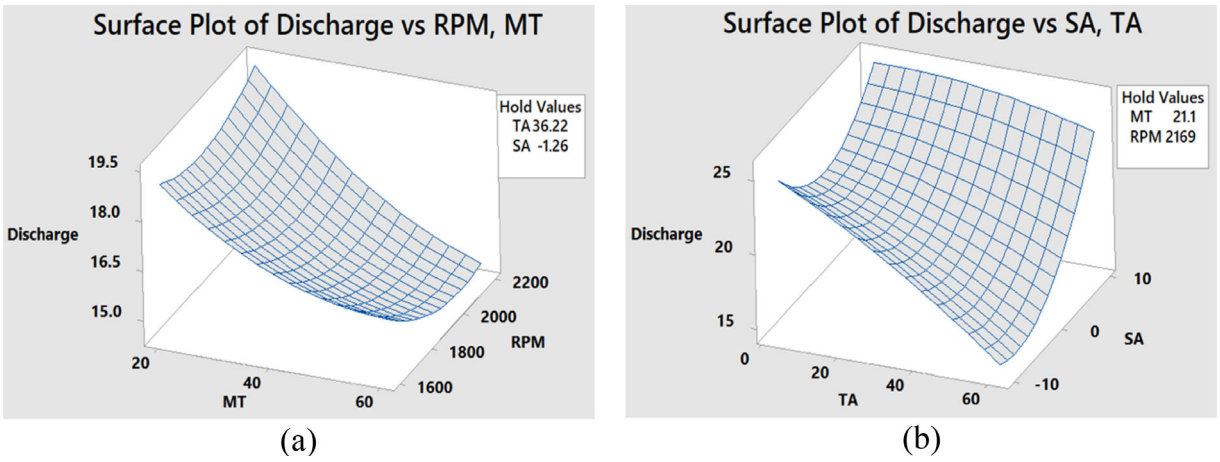

FIGURE 9 Variation of pump discharge.

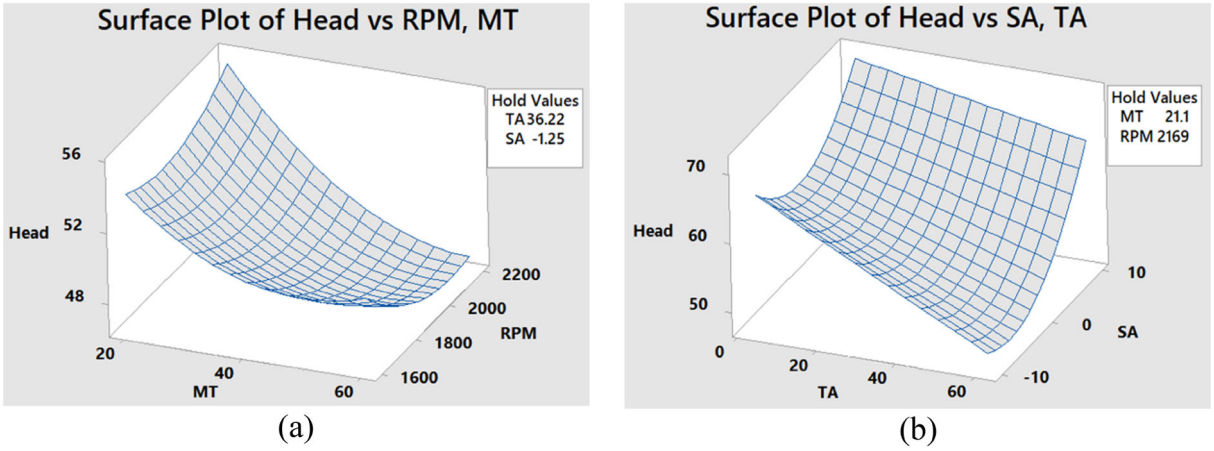

FIGURE 10 Variations of developed head with the MT, TA, SA, and RPM.

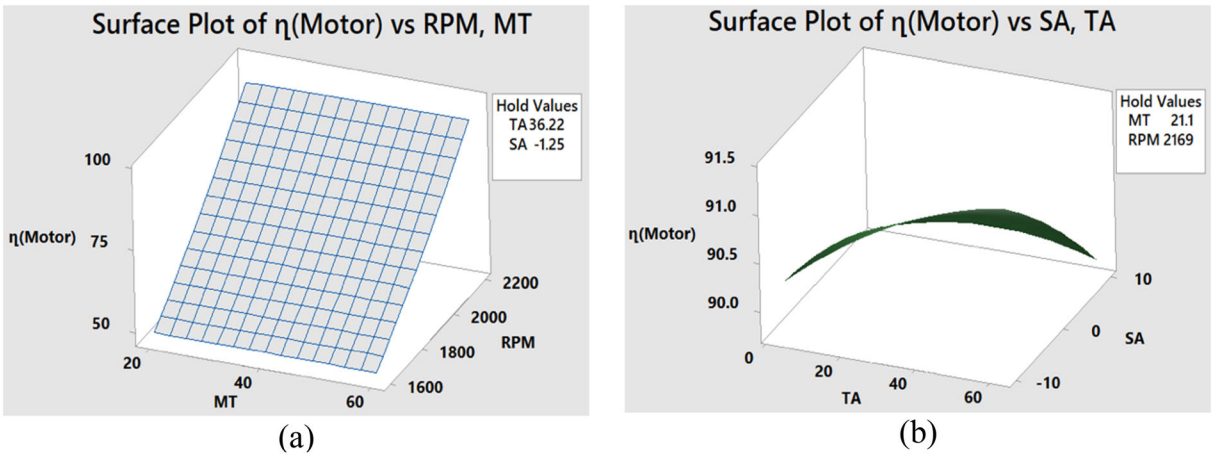

FIGURE 11 Variation of motor efficiency with the MT, SA, TA, and RPM of the motor.

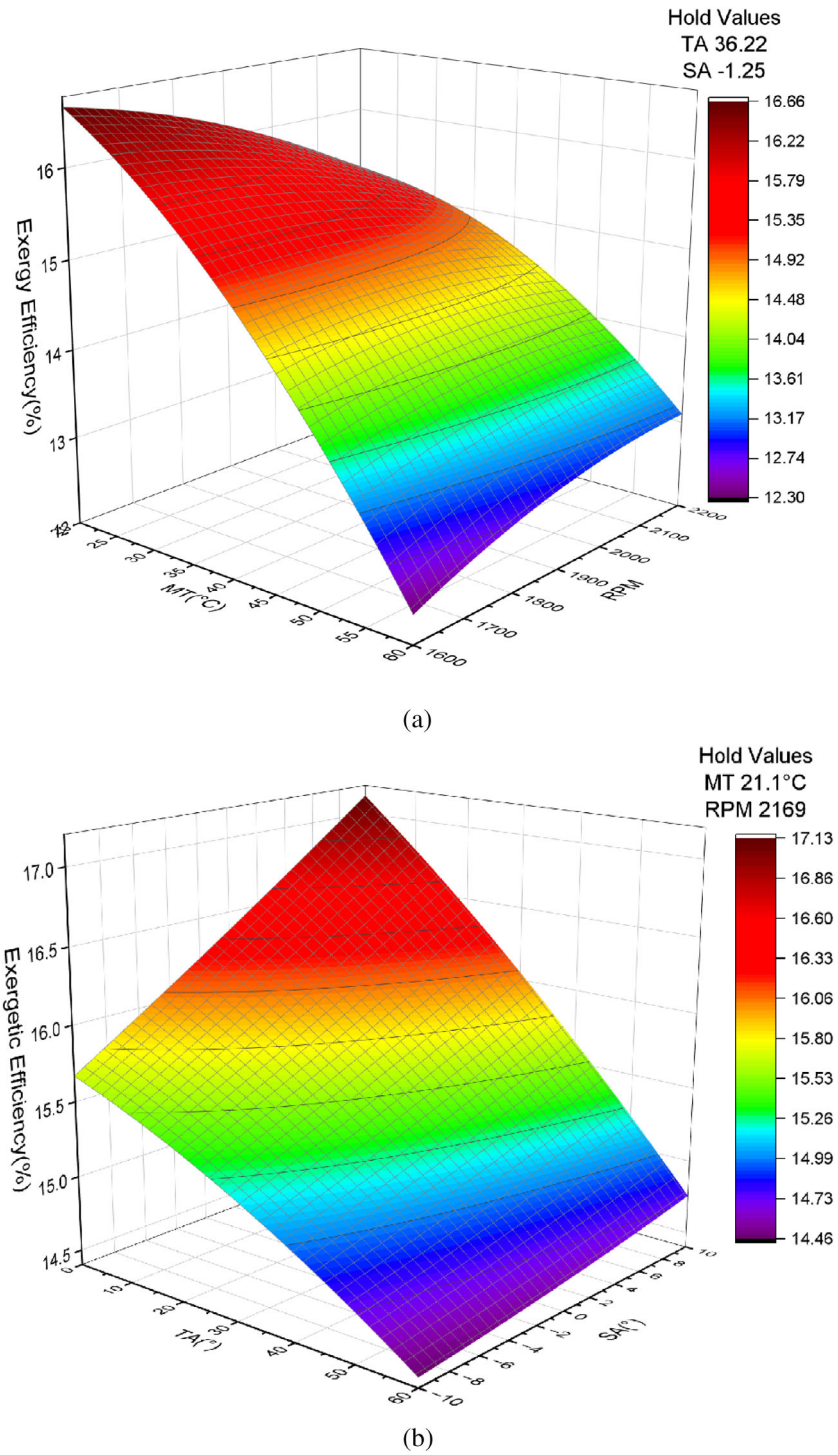

FIGURE 12 Exergetic efficiency variation with SA, TA, RPM, and MT.

4.7 | Interactive effect of various input factors on LCOE

$$LCOE = -0.1793 - 0.000120\,\alpha - 0.00106\,\lambda + 0.001171\,T_m - 0.000205\,N - 0.000007\,\alpha^2 - 0.000096\,\lambda^2 - 0.000021\,T_m - 0.000000\,N^2 + 0.000004\,\alpha\lambda + 0.000005\,\alpha T_m + 0.00000\,\alpha N - 0.0000007\,\lambda T_m - 0.000000\,\lambda N - 0.00000\,T_m N \quad (9)$$

The LCOE is the most important parameter in the solar pump project, it is the ratio of the cost incurred in the project and the total power produced by the solar pump. So, if the power produced by the solar pump is maximum throughout the year, then LCOE is minimum. Figure 13a,b shows how the LCOE is changed with the variation of TA, SA, MT, and RPM of the pump. Figure 13a shows that an initially increase in the value of MT increases LCOE and reached the maximum and a further increase in the value of MT reduces the LCOE. Figure 13a shows that if the pump runs at higher RPM the pump life is reduced and LCOE is increased. So small magnitude of MT and low RPM reduced the LCOE of the solar pump. Figure 13b represents the effect of TA and SA on the LCOE of the solar pump system. Figure 13b shows that if TA

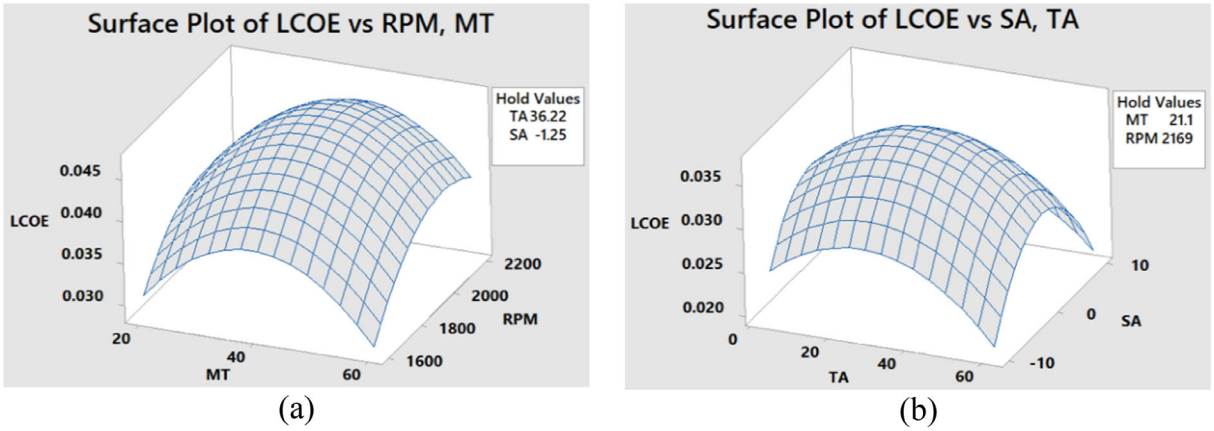

FIGURE 13 LCOE variation with the TA, SA, MT, and RPM.

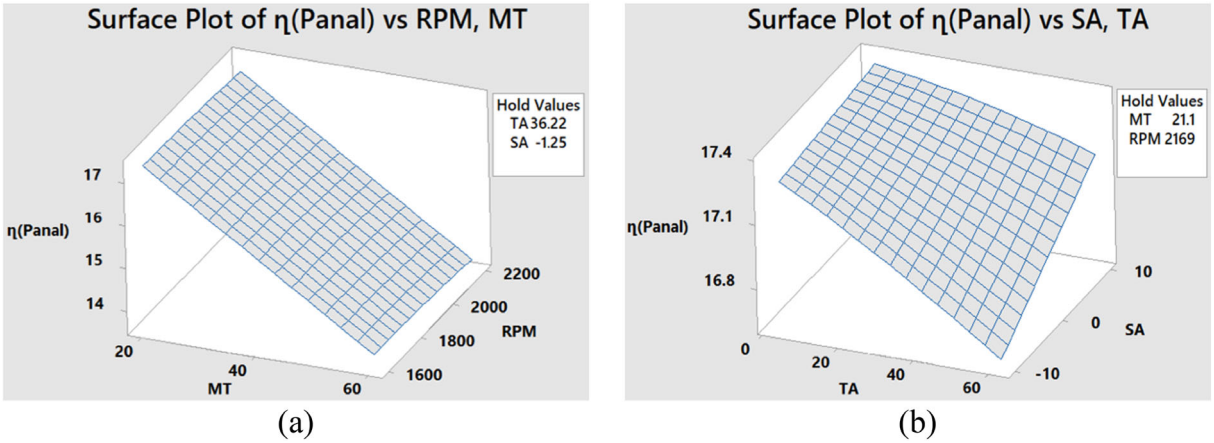

FIGURE 14 Solar panel efficiency variation with input variables.

increases then LCOE increases and reached a maximum level further increase in the value of TA reduced the LCOE.[35] Figure 13b shows that the small value of TA and the low value of SA give the minimum LCOE.

4.8 | Interactive effect of various input factors on η (panel)

$$\eta_P = 17.34 + 0.01827\,\alpha - 0.0411\,\lambda - 0.1\,T_m + 0.001880\,N - 0.000029\,\alpha^2 + 0.000004\,\lambda^2 + 0.000013\,T_m - 0.00000\,N^2 + 0.000354\,\alpha\lambda + 0.000248\,\alpha T_m - 0.000014\,\alpha N - 0.000547\,\lambda T_m + 0.000025\,\lambda N + 0.000001\,T_m N \quad (10)$$

Figure 14a represents the variation of solar panel efficiency with the MT and RPM at holding the value of TA 36.22 and SA −1.25. Figure 14a shows that if the MT value increases then the solar panel efficiency is reduced continuously since increasing MT enhances the energy losses in the atmosphere.[48] The efficiency of the solar panel remains constant by increasing and decreasing the value of the speed of the pump. Figure 14b shows that increasing the value of TA reduced the solar panel efficiency due to an increase in values of TA reduced the power produced by solar panels and a reduction in values of SA increase the solar panel efficiency by holding MT 21.1°C and RPM 2169.

4.9 | Interactive effect of various input factors on η (overall)

$$\eta_O = 11.04 - 0.0169\,\alpha - 0.0747\,\lambda - 0.0694\,T_m - 0.00865\,N - 0.000329\,\alpha^2 - 0.001133\,\lambda^2 - 0.000283\,T_m^2 + 0.00005\,N^2 + 0.000412\,\alpha\lambda + 0.00317\,\alpha T_m + 0.000010\,\alpha N + 0.000631\,\lambda T_m + 0.000018\,\lambda N + 0.000016\,T_m N \quad (11)$$

The overall efficiency is the multiplication of solar panel efficiency and pumps efficiency. The variation of the overall efficiency versus MT, RPM, TA, and SA is shown in Figure 15. Figure 15a shows that increasing the value of MT reduced the overall efficiency due to high values of MT enhancing the heat loss in the atmosphere but if the RPM of the motor increases the overall efficiency is enhanced since the pump produced more power. Figure 15b shows that if TA values increase then the overall efficiency is reduced but the increment in

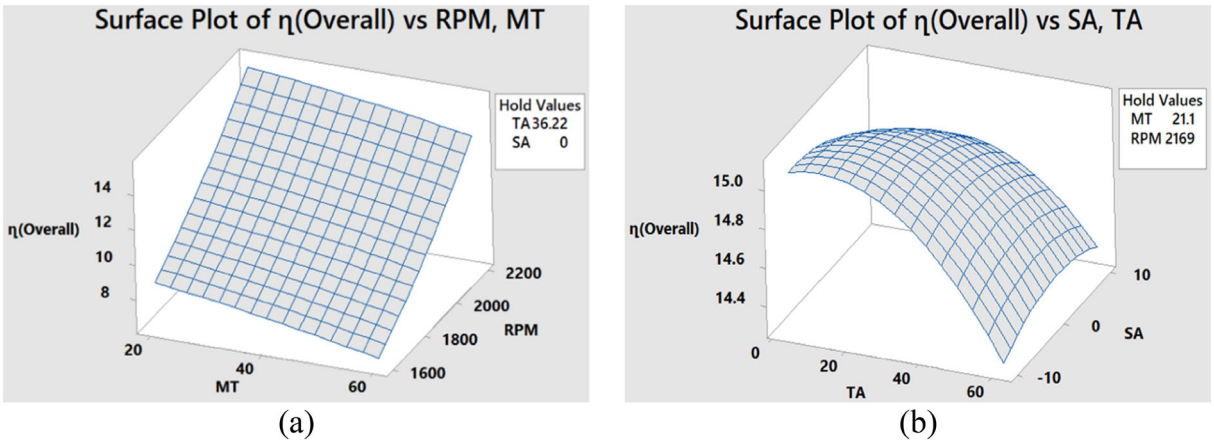

FIGURE 15 Variation of the overall efficiency of the solar pump with the TA, SA, MT, and RPM.

TABLE 11 The verification test of output response.

	Predicted value	Experimental value	Error (%)
SF	728 W/m^2	737.6 W/m^2	3.2%
Power O/P	3661.4578 W	3555.27 W	2.9%
Discharge	19.2681 m^3/hr	18.59 m^3/hr	3.5%
Head	55.17 m	53.5149 m	3%
η (Motor)	90.7488%	88.5617%	2.41%
Exergy efficiency	15.3799%	14.9954%	2.5%
LCOE	0.0361 $/KWh	0.0350892 $/KWh	2.8%
η (Panel)	17.1774%	16.737%	2.56%
η (Overall)	15.0117%	14.4337%	3.85%

Note: TA (62°), SA (−1.250°), MT (20°C), and RPM (2169.69).

values of SA enhanced the overall efficiency at holding the values of MT 21.1°C and speed 2169 rpm.

5 | ERROR DESCRIPTIONS

The ANOVA analyses give the error description in a solar power water pump system. The tests were conducted by varying of tilt angle, the surface azimuthal angle, modular temperature, and rpm of the motor. The optimum value of input factors is TA (62°), SA (−1.250°), MT (20°C), and rpm (2169.69). Three confirmation tests were carried out to validate the RSM predictions, and their mean is taken into account. Table 11 shows the detail of the experiments. solar flux, power output discharge (m^3/s), head required, motor efficiency (%), exergy, LCOE, panel efficiency (%), and overall efficiency (%) responses were measured experimentally. These experimental findings were then compared to the RSM model's predictions. The % error for solar flux, power output, discharge (m^3/s), head required, motor efficiency (%), exergy, LCOE, panel efficiency (%), and overall efficiency (%) is shown in Table 11. The average inaccuracy for solar flux, power output discharge (m^3/s), head required, motor efficiency (%), exergy, LCOE, panel efficiency (%), and overall efficiency (%) is 3.2467% respectively, which are substantially below permissible limits.

6 | CONCLUSIONS

This article focused on optimizing the performance of the solar pump based on the main input parameters like TA, SA, MT and the Speed of the motor. For optimization purpose Response Surface Methodology tool has been used. The following outcomes were made through the experimental investigation and optimization techniques:

- The statistical analysis contributed to finding the significant parameters that had the largest impact on the output characteristics, and the Design of Experiments (DoE) based on RSM was incredibly valuable in planning the experiment. This DoE reduced the time by reducing the number of tests required and represented all data using statistically established models.
- Based on the optimization of experimental data and data generated by the model equation by RSM, it is concluded that the optimum value of input parameters are TA (36.22°), SA (−1.25°), MT (20°C), and RPM (2169.69).
- On the optimum setting of input parameters, the values of the response are maximum SF (728 W/m^2), maximum power output (3661.4578 W), minimum discharge (19.2681 m^3/h), head developed (55.17 m), maximum motor efficiency (90.7488%), maximum

exergetic efficiency (15.3799%), minimum LCOE (0.0361 $/KWh), maximum panel efficiency (17.1774%) and maximum overall efficiency (15.0117%).

- The desirability effect of this model was obtained at 72.27%. All of the produced regression models for solar flux, power output, discharge (m^3/h), head required, motor efficiency (%), exergy, LCOE, panel efficiency (%), and overall efficiency (%) were found to be statistically significant at the 95% confidence level.
- The ANOVA study revealed that the equivalent values of R^2 (86.21%, 89.35%, 91.47%, 98.77%, 99.99%, 97.82%, 78.63%, 99.85%, and 99.82%) for solar flux, power output discharge (m^3/h), head required, motor efficiency (%), exergy, LCOE, panel efficiency (%), and overall efficiency (%) respectively and adjusted R^2 in the current model suggests that the present proposed model could be effectively matched with the experimental outcomes.
- The *P* values of the ANOVA analysis represent the probability of uncertainty, it was found to be less than 0.05 in most of the responses outcomes, Which shows the validity of the ANOVA regression model to the satisfactory.

NOMENCLATURE

Variable	Description
P_O	Power output. (W).
Q	Discharge. (m^3/h).
H_R	Head developed (m).
η_m	Motor efficiency (%).
η_p	Solar panel efficiency (%).
ϕ	Exergetic efficiency (%).
η_O	Overall efficiency (%).
α	Tilt angle (°)
λ	Surface azimuth angle (°)
T_m	Module temperature (°C)
N	Speed of the pump (RPM)
I_t	Solar flux (W/m^2)

AUTHOR CONTRIBUTIONS

Manoj Kumar Singh: Conceptualization; data curation; formal analysis; funding acquisition; investigation; methodology; project administration.

ACKNOWLEDGMENTS

This work was supported by the collaborative project scheme (CRS) fund under the NATIONAL PROJECT IMPLEMENTATION UNIT (NPIU) (A Unit of MHRD, Govt. of India for Implementation of World Bank Assisted Projects in Technical Education) [CRS Project ID: 1-5736521897].

DATA AVAILABILITY STATEMENT

Data is given in the manuscript in Table 4.

ORCID

Vineet Singh https://orcid.org/0000-0003-3328-2588

REFERENCES

1. Business Opportunities in India. *Investment Ideas, Industry Research*. IBEF; 2022 https://www.ibef.org/
2. A. Ismail, "*Solar Water Pump System*," Greenstream Publishing; 2012. http://www.ee.ic.ac.uk/mateusz.lisewski10/yr2proj/images/Tsavos_Thirsty_Report.pdf.
3. Hamidat A, Benyoucef B, Hartani T. Small-scale irrigation with photovoltaic water pumping system in Sahara regions. *Renew Energy*. 2003; 28(7):1081-1096. doi:10.1016/S0960-1481(02)00058-7
4. Daud AK, Mahmoud MM. Solar powered induction motor-driven water pump operating on a desert well, simulation and field tests. *Renew Energy*. 2005;30(5):701-714. doi:10.1016/J.RENENE.2004.02.016
5. Eshra NM, Salem MG. Solar energy application in drainage pumping stations to save water and reducing CO_2 emission. *Energy Rep*. 2020; 6:354-366. doi:10.1016/J.EGYR.2020.08.056
6. Closas A, Rap E. Solar-based groundwater pumping for irrigation: sustainability, policies, and limitations. *Energy Policy*. 2017;104:33-37. doi:10.1016/J.ENPOL.2017.01.035
7. Kumar A, Kumar K, Kaushik N, Sharma S, Mishra S. Renewable energy in India: current status and future potentials. *Renew Sustain Energy Rev*. 2010;14(8):2434-2442. doi:10.1016/J.RSER.2010.04.003
8. Spencer LC. A comprehensive review of small solar-powered heat engines: part I. A history of solar-powered devices up to 1950. *Sol Energy*. 1989;43(4):191-196. doi:10.1016/0038-092X(89)90019-4
9. Smulders PT, de Jongh J. Wind water pumping: status, prospects and barriers. *Renew Energy*. 1994;5(1–4):587-594. doi:10.1016/0960-1481(94)90440-5
10. Ramadhas AS, Jayaraj S, Muraleedharan C. Power generation using coir-pith and wood derived producer gas in diesel engines. *Fuel Process Technol*. 2006;87(10):849-853. doi:10.1016/J.FUPROC.2005.06.003
11. Manolis EN, Zagas TD, Karetsos GK, Poravou CA. Ecological restrictions in forest biomass extraction for a sustainable renewable energy production. *Renew Sustain Energy Rev*. 2019;110:290-297. doi:10.1016/J.RSER.2019.04.078
12. Rohit KB, Karve GM. International journal of emerging technology and advanced engineering solar water pumping system. *Certif J*. 2008;9001(7):323 www.ijetae.com
13. Sontake VC, Kalamkar VR. Solar photovoltaic water pumping system – a comprehensive review. *Renew Sustain Energy Rev*. 2016; 59:1038-1067. doi:10.1016/J.RSER.2016.01.021
14. Bekraoui A, Yaichi M, Allali M, Taybi A, Boutadara A. Performance of photovoltaic water pumping system LN Adrar, Algeria. *6th Int Renew Sustain Energy Conf IRSEC*. 2018;1-5. doi:10.1109/IRSEC.2018.8702990
15. Kolhe M, Joshi JC. Performance analysis of directly coupled photovoltaic electro-mechanical systems. 2005;216(6):453-464. doi:10.1243/095765002761034221
16. Chaurey A, Sadaphal PM, Tyaqi D. Experiences with SPV water pumping systems for rural applications in India. *Renew Energy*. 1993; 3(8):961-964. doi:10.1016/0960-1481(93)90058-O
17. Rout A, Singh S, Mohapatra T, Sahoo SS, Solanki CS. Energy, exergy, and economic analysis of an off-grid solar polygeneration system. *Energy Convers Manage*. 2021;238:114177. doi:10.1016/j.enconman.2021.114177
18. Allouhi A, Buker MS, el-houari H, et al. PV water pumping systems for domestic uses in remote areas: sizing process, simulation and economic evaluation. *Renew Energy*. 2019;132:798-812. doi:10.1016/J.RENENE.2018.08.019
19. Sado KA, Hassan LH, Moghavvemi M. Design of a PV-powered DC water pump system for irrigation: a case study. *53rd Int Univ Power Eng Conf UPEC*. 2018;10:1-6. doi:10.1109/UPEC.2018.8542072
20. Kaldellis JK, Meidanis E, Zafirakis D. Experimental energy analysis of a stand-alone photovoltaic-based water pumping installation. *Appl Energy*. 2011;88(12):4556-4562. doi:10.1016/J.APENERGY.2011.05.036

21. Raymond M. *Solar-Energy-System Performance Evaluation: Honeywell Salt River Project*, Phoenix Publishing Group, Arizona; 1982. doi:10.2172/6028904
22. Thomas S, Sahoo SS, Ajithkumar G, Thomas S, Rout A, Mahapatra SK. Socio-economic and environmental analysis on solar thermal energy-based polygeneration system for rural livelihoods applications on an Island through interventions in the energy-water-food nexus. *Energy Convers Manag*. 2022;270(1):116235. doi:10.1016/j.enconman.2022.116235
23. Le Roux WG. Optimum tilt and azimuth angles for fixed solar collectors in South Africa using measured data. *Renew Energy*. 2016;96:603-612. doi:10.1016/J.RENENE.2016.05.003
24. Elnozahy MS, Salama MMA. Technical impacts of grid-connected photovoltaic systems on electrical networks—a review. *J Renew Sustain Energy*. 2013;5(3):032702. doi:10.1063/1.4808264
25. Huang CM, Chen SJ, Yang SP, Kuo CJ. One-day-ahead hourly forecasting for photovoltaic power generation using an intelligent method with weather-based forecasting models. *IET Gener Transm Distrib*. 2015;9(14):1874-1882. doi:10.1049/IET-GTD.2015.0175
26. Li G, Jin Y, Akram MW, Chen X. Research and current status of the solar photovoltaic water pumping system – a review. *Renew Sustain Energy Rev*. 2016;79:440-458. doi:10.1016/j.rser.2017.05.055
27. Sci-Hub. Experimental investigations on the seasonal performance variations of directly coupled solar photovoltaic water pumping system using centrifugal pump. *Environ Dev Sustain*. 2020;23(6):8288-8306. doi:10.1007/s10668-020-00965-x
28. Tiwari AK, Sontake VC, Kalamkar VR. Enhancing the performance of solar photovoltaic water pumping system by water cooling over and below the photovoltaic array. *J Sol Energy Eng Trans ASME*. 2020;142(2):1-9. doi:10.1115/1.4044978/1031132
29. Amer EH, Younes MA. Estimating the monthly discharge of a photovoltaic water pumping system: model verification. *Energ Conver Manage*. 2006;47(15–16):2092-2102. doi:10.1016/J.ENCONMAN.2005.12.001
30. Mohapatra T, Padhi BN, Sahoo SS. Analytical investigation and performance optimization of a three fluid heat exchanger with helical coil insertion for simultaneous space heating and water heating. *Heat Mass Transf Und Stoffuebertragung*. 2019;55(6):1723-1740. doi:10.1007/s00231-018-02545-2
31. Rout A, Sahoo SS, Singh S, Pattnaik S, Barik AK, Awad MM. Benefit-cost analysis and parametric optimization using Taguchi method for a solar water heater. *Des Perform Optim Renew Energy Syst*. 2021;6:101-116. doi:10.1016/B978-0-12-821602-6.00008-0
32. Singh V, Yadav VS. Application of RSM to optimize solar pump LCOE and power output. *IETE J Res*. 2022;10:2069165. doi:10.1080/03772063.2022.2069165
33. Singh V, Yadav VS. Optimizing the performance of solar panel cooling apparatus by application of response surface methodology. *Sage J*. 2022;236:1-18. doi:10.1177/09544062221101828
34. Sci-Hub. Pumped Storage-Based Standalone Photovoltaic Power Generation System: Modeling and Techno-Economic Optimization. *Appl Energy*. 2015;137:649-659. doi:10.1016/j.apenergy.2014.06.005
35. Campana PE, Li H, Zhang J, Zhang R, Liu J, Yan J. Economic optimization of photovoltaic water pumping systems for irrigation. *Energ Conver Manage*. 2015;95:32-41. doi:10.1016/J.ENCONMAN.2015.01.066
36. Ba A, Aroudam E, Chighali OE, Hamdoun O, Mohamed ML. Performance optimization of the PV pumping system. *Procedia Manuf*. 2018;22:788-795. doi:10.1016/J.PROMFG.2018.03.112
37. Bhayo BA, Al-Kayiem HH, Gilani SIU, Ismail FB. Power management optimization of hybrid solar photovoltaic-battery integrated with pumped-hydro-storage system for standalone electricity generation. *Energ Conver Manage*. 2020;215:112942. doi:10.1016/J.ENCONMAN.2020.112942
38. Merei G, Berger C, Sauer DU. Optimization of an off-grid hybrid PV–wind–diesel system with different battery technologies using genetic algorithm. *Sol Energy*. 2013;97:460-473. doi:10.1016/J.SOLENER.2013.08.016
39. Sanaye S, Hajabdollahi H. Thermo-economic optimization of solar CCHP using both genetic and particle swarm algorithms. *J Sol Energy Eng Trans ASME*. 2015;137(1):1-11. doi:10.1115/1.4027932/379583
40. Kumar NM, Vishnupriyan J, Sundaramoorthi P. Techno-economic optimization and real-time comparison of sun tracking photovoltaic system for rural healthcare building. *J Renew Sustain Energy*. 2019;11(1):015301. doi:10.1063/1.5065366
41. Khan A, Khan R. Cost optimization of hybrid microgrid using solar PV, fuel cell and diesel generator in HOMER. *Conf Energy Conserv Effic Proc*. 2018;8:14-18. doi:10.1109/ECE.2018.8554974
42. Pali BS, Vadhera S. Uninterrupted sustainable power generation at constant voltage using solar photovoltaic with pumped storage. *Sustain Energy Technol Assess*. 2020;42:100890. doi:10.1016/j.seta.2020.100890
43. Chelladurai SJS, Arthanari R. Effect of stir cast process parameters on wear behaviour of copper coated short steel fibers reinforced LM13 aluminium alloy composites. *Mater Res Express*. 2018;5(6):066550. doi:10.1088/2053-1591/AACD38
44. Hatami M, Jing D. Optimization of wavy direct absorber solar collector (WDASC) using Al2O3-water nanofluid and RSM analysis. *Appl Therm Eng*. 2017;121:1040-1050. doi:10.1016/J.APPLTHERMALENG.2017.04.137
45. Katekaew S, Suiuay C, Senawong K, Seithtanabutara V, Intravised K, Laloon K. Optimization of performance and exhaust emissions of single-cylinder diesel engines fueled by blending diesel-like fuel from Yang-hard resin with waste cooking oil biodiesel via response surface methodology. *Fuel*. 2021;304:121434. doi:10.1016/J.FUEL.2021.121434
46. Li D, Li Y, Asadizadeh M, Masoumi H, Hagan PC, Saydam S. Assessing the mechanical performance of different cable bolts based on design of experiments techniques and analysis of variance. *Int J Rock Mech min Sci*. 2020;130:104307. doi:10.1016/J.IJRMMS.2020.104307
47. Thomas SJ, Thomas S, Sahoo SS, Gobinath R, Awad MM. Allotment of waste and degraded land parcels for PV based solar parks in India: effects on power generation cost and influence on investment decision-making. *Sustain*. 2022;14(3):178-184. doi:10.3390/su14031786
48. Gad HE. PERFORMANCE PREDICTION OF A PROPOSED PHOTOVOLTAIC WATER PUMPING SYSTEM AT SOUTH SINAI, EGYPT CLIMATE CONDITIONS. 2009.
49. Yesildal F, Ozakin AN, Yakut K. Optimization of operational parameters for a photovoltaic panel cooled by spray cooling. *Eng Sci Technol an Int J*. 2022;25:100983. doi:10.1016/J.JESTCH.2021.04.002
50. Belgacem BG. Performance of submersible PV water pumping systems in Tunisia. *Energy Sustain Dev*. 2012;16(4):415-420. doi:10.1016/J.ESD.2012.10.003

How to cite this article: Singh V, Yadav VS, Trivedi V, Singh MK. Performance optimization of solar pump operating by PV module. *Environ Prog Sustainable Energy*. 2023;e14293. doi:10.1002/ep.14293